Selective and potent PROTAC degraders of c-Src kinase

Wuxiang Mao,[a] Nathalie M. Vandecan,[a] Christopher R. Bingham,[a] Pui Ki Tsang,[a] Peter Ulintz,[b] Rachel Sexton,[a] Daniel A. Bochar,[a] Sofia D. Merajver,[b] and Matthew B. Soellner*,[a,b]

a. Department of Chemistry, University of Michigan, 930 N. University Ave., Ann Arbor, MI, 48109.
b. Department of Internal Medicine, University of Michigan, 1500 E. Medical Ave., Ann Arbor, MI 48109.

Abstract

Using dasatinib linked to E3 ligase ligands, we identified a potent and selective dual Csk/c-Src PROTAC degrader. We then replaced dasatinib the c-Src directed ligand with a conformation-selective analog that stabilizes the αC-helix out conformation of c-Src. Using the αC-helix out ligand, we identified a PROTAC that is potent and selective for c-Src. Using our c-Src PROTACs, we identified pharmacological advantages to c-Src degradation compared to inhibition with respect to cancer cell proliferation.

Introduction

Protein kinases (PKs) play an essential role in cell signaling and in the regulation of key biological processes, including proliferation, differentiation, and apoptosis [1–3]. For many kinases, there are divergent effects on cellular signaling between genomic knockdown (e.g., siRNA) and pharmacological intervention with kinase inhibitors [4–6]. This disconnect between genomic and pharmacological intervention are presumed to be due to noncatalytic functions of kinases being disrupted only by genomic knockdown [4–6]. Kinase-directed PROTACs thus represent a potential advance in targeting kinases for which non-catalytic functions are important for cell signaling.

c-Src, a tyrosine kinase, was the first proto-oncogene discovered and is frequently over-expressed in cancers [7–9]. While the mechanisms remain poorly understood [9], the extent of c-Src over-expression often correlates with the metastatic potential of the malignant tumor and inhibition of c-Src has been shown to decrease breast cancer metastases in mice [10]. c-Src was validated as a target for many solid tumors via genetic knockdown; however, pharmacological inhibition (both in the clinic and in pre-clinical models) leads to a signaling phenotype that is divergent from genetic knockdown [10]. Upon knockdown (e.g., with siRNA), triple negative breast cancer (TNBC) and basal bladder cancers exhibit decreased proliferation and invasion properties [10,11]. Unfortunately, studies with small molecule inhibitors of c-Src (including: dasatinib, bosutinib, and ponatinib), failed to recapitulate the strong anti-cancer phenotype observed from genetic knockdown of c-Src, and were not successful in the clinic [10,11]. PROTACs provide a means of chemical knockdown [12], and we were thus interested in developing a PROTAC for c-Src.

Results and Discussion

Design and evaluation of c-Src directed PROTACs. To identify a PROTAC for c-Src, we envisioned combining dasatinib, a potent c-Src/Abl kinase inhibitor, with thalidomide, a cereblon E3 ligase ligand. Dasatinib based PROTACs have been reported for degrading c-Abl and Bcr-Abl, including **DAS-6-2-2-6** (Figure 1) [13]. We were hopeful that **DAS-6-2-2-6** would be able to degrade c-Src, but we observed no degradation of c-Src in CAL148 cells (100 nM at 18 hours). Consistent with PROTAC literature on linker design [14], we hypothesized that the flexible and long linker found in **DAS-6-2-2-6** is not appropriate for degrading c-Src.

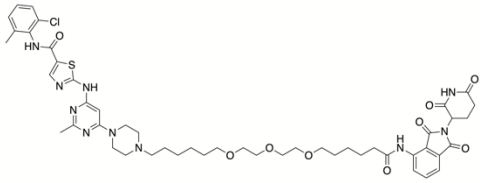

DAS-6-2-2-6-CRBN

66% Bcr-Abl degraded (100 nM, 18h; KCL22 cells)
0% c-Src degraded (100 nM; 18h; CAL148 cells)

Figure 1. DAS-6-2-2-6-CRBN is a previously reported PROTAC degrader of Bcr-Abl. We found that **DAS-6-2-2-6** is capable of degrading Bcr-Abl, but does not degrade c-Src.

Thus, we connected dasatinib to a thalidomide-based ligand using shorter and conformationally constrained linkers. We also explored the linker connection-site to thalidomide (ortho- vs meta- linkage, Figure 2). Using a biochemical activity assay for c-Src kinase activity [15], we found that each dasatinib-based PROTACs was a potent inhibitor of c-Src (IC_{50} < 100 nM at 1 mM ATP) (Supplementary Table S1). Using a commercially available cell-based binding assay (Promega NanoBRET, [16]) we found that each dasatinib-based PROTAC was a competent cellular binder of both c-Src and cereblon (Supplementary Table S1).

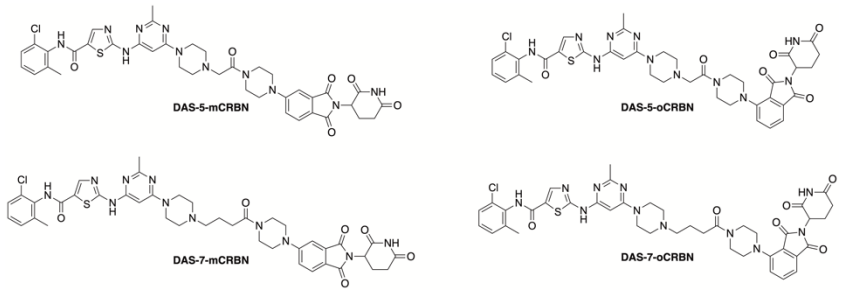

Figure 2. Putative c-Src PROTACs based on dasatinib and thalidomide.

Our dasatinib-based PROTACs were evaluated for their ability to degrade c-Src in a cellular context (Table 1). CAL148 cells were treated with 100 nM compound for 18 hours and the amount of c-Src was quantified using a total protein c-Src ELISA. We selected CAL148 cells for the initial screen because CAL148 cells have detectable c-Src protein levels, however, are not growth-sensitive to c-Src knockdown [17]. Using our total protein c-Src ELISA, we found that all dasatinib-based PROTACs cause significant degradation of c-Src (Table 1). We determined the ability to degrade c-Src in a dose-dependent manner and found that each c-Src PROTAC was a potent degrader (Table 1).

Table 1. Degradation of c-Src and c-Abl by dasatinib-based PROTACs.

	% c-Src degraded (100 nM, 18 h)[a]	c-Src DC_{50}, (18 h)[a]	% Bcr-Abl degraded (100 nM, 18 h)[b]
DAS-5-mCRBN	86%	5 nM	68%
DAS-7-mCRBN	86%	0.8 nM	79%
DAS-5-oCRBN	78%	3 nM	4%
DAS-7-oCRBN	86%	1 nM	66%

[a] CAL-148 cell line, [b] KCL-22 cell line

To confirm that the observed degradation is mediated by ubiquitination and proteosomal degradation, we measured the amount of c-Src remaining in the presence and absence of 1 μM bortezomib (proteasome inhibitor) and 10 μM pomalidomide (a ligand of cereblon). To confirm the degradation requires binding to the ATP-site of c-Src, we added 1 μM DGY-06-116 (an irreversible inhibitor of c-Src [18]) prior to incubation with **DAS-5-oCRBN**. We found that each of these conditions prevents degradation of c-Src by 100 nM **DAS-5-oCRBN**, confirming that degradation is mediated by ubiquitination and proteasomal degradation of c-Src (Figure 3).

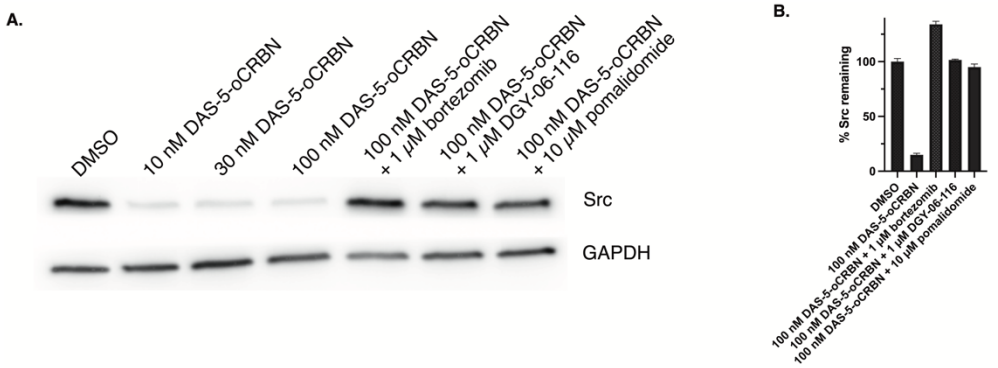

Figure 3. A. c-Src PROTACs require binding to both E3 ligase and c-Src for cellular degradation of c-Src. Uncropped blot can be found in Supporting Information. B. Quantitative ELISA results demonstrate that DAS-5-oCRBN requires both ligase and kinase engagement for c-Src degradation.

It has been previously reported that methylation of the glutarimide of thalidomide prevents binding to cereblon [22]. Thus, we synthesized an inactive analog of **DAS-5-oCRBN** that should be incapable of binding cereblon (**DAS-5-oCRBN-NMe**). Consistent with prior reports, we found that **DAS-5-oCRBN-NMe** does not bind cereblon (Supplementary Figure 1).

Assessing the selectivity of c-Src PROTACs. Dasatinib is a pan-tyrosine kinase inhibitor [19]; however, selective PROTAC-based degradation has been reported for PROTACs synthesized using promiscuous kinase inhibitors [14]. In addition to c-Src, dasatinib is a potent inhibitor of Bcr-Abl kinase [19]. Moreover, dasatinib-based PROTACs have previously been reported that target c-Abl and Bcr-Abl (Figure 1) [13]. Thus, degradation of Bcr-Abl represents a meaningful initial measure of selectivity for our c-Src PROTACs.

Using an ELISA for Bcr-Abl we determined the amount of Bcr-Abl degraded by our PROTACs after treatment of KCL-22 cells with 100 nM compound for 18 hours. KCL-22 is a Bcr-Abl transformed chronic myelogenous leukemia cell line [20]. Using our ELISA for Bcr-Abl, we found that **DAS-5-oCRBN** was uniquely selective for degrading c-Src over c-Abl (Table 1). Our results demonstrate that that the cereblon ligand trajectory (4-amino- versus 5-amino-thalidomide) can dramatically impact which kinase(s) are degraded. We determined the c-Src and Bcr-Abl DC_{50} values for **DAS-5-oCRBN** in KCL22 cells (Figure 4).

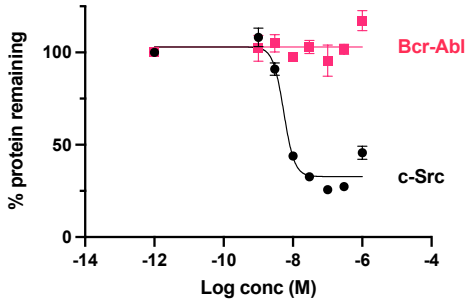

Figure 4. DAS-5-oCRBN is a selective degrader of c-Src over Bcr-Abl in KCL22 cell line.

Given that we observed selectivity for c-Src over Abl degradation, we wanted to more broadly determine the degradation profile of **DAS-5-oCRBN**. We used reverse-phase protein arrays (RPPA) to quantify the level remaining of 394 cancer-related proteins (Supplementary Figure S2) [21]. In the RPPA panel, **DAS-5-oCRBN** significantly (>50% degradation) degraded only Csk and c-Src. Csk is a known off-target of dasatinib [19].

Conformation-selective c-Src PROTACs. We previously reported 'conformation-selective' analogs of dasatinib that modulate the global conformation of c-Src [23,24]. **DAS-CHO-II** is an αC-helix out analog of dasatinib that stabilizes the closed global conformation of c-Src [23,24]. In addition to altering the conformational dynamics of c-Src, **DAS-CHO-II** also has improved kinome-wide selectivity for c-Src compared to dasatinib [23].

We synthesized **DAS-CHO-5-oCRBN** and determined the kinome binding profile for both **DAS-CHO-5-oCRBN** and **DAS-5-oCRBN** against 176 diverse kinases (500 nM each compound, Luceome Biotechnologies, Tucson,

AZ). Consistent with our previous report for dasatinib and **DAS-CHO-II** [23], we found that **DAS-CHO-5-oCRBN** is more selective than **DAS-5-oCRBN** (Figure 5).

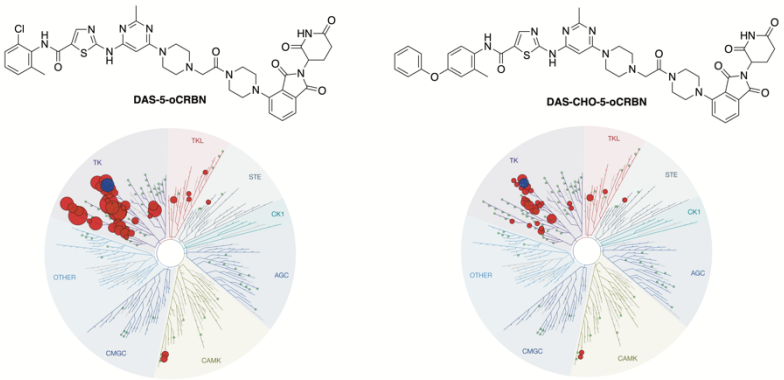

Figure 5. Kinome-wide selectivity of **DAS-5-oCRBN** and Das-CHO-based **DAS-CHO-5-oCRBN**.

In the RPPA panel, **DAS-CHO-5-oCRBN** only significantly (>50% degradation) degraded c-Src (Supplementary Figure S1). We confirmed the high degree of selectivity using a quantitative proteomics experiment in CAL148 cells where only c-Src was observed to be significantly degraded (Figure 6).

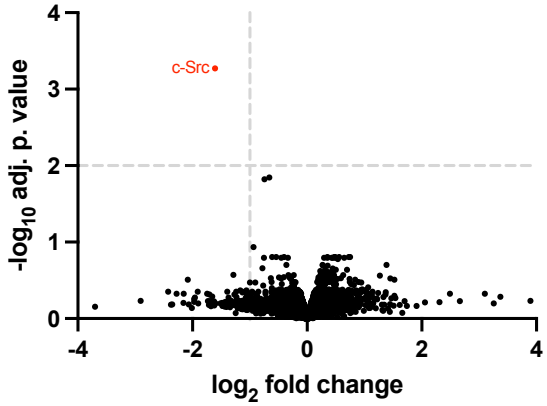

Figure 6. Volcano plot of quantitative proteomics experiment of proteins degraded by **DAS-CHO-5-oCRBN** (100 nM, 18 h, n=3) in CAL148 cells.

We next determined the DC_{50} (using ELISA, Supplementary Figures S3–S6) and D_{max} (using Western blot, Supplementary Table S3) for **DAS-5-oCRBN** and **DAS-CHO-5-oCRBN** across four cell lines (CAL148, KCL22, MDA-MB-231, and SUM51) (Table 2). While **DAS-CHO-5-oCRBN** is a more selective degrader (see above), **DAS-5-oCRBN** is a more potent degrader of c-Src. Across the four cell lines, **DAS-5-oCRBN** has an average DC_{50} = 7 nM and average D_{max} = 92% while **DAS-CHO-5-oCRBN** has an average DC_{50} = 55 nM and average D_{max} = 80%.

Table 2. Degradation of c-Src by conformation-selective PROTACs.

	DAS-5-oCRBN DC_{50} (D_{max})	**DAS-CHO-5-oCRBN** DC_{50} (D_{max})
CAL148	4 nM (95%)	62 nM (93%)
KCL22	5 nM (91%)	70 nM (92%)
MDA-MB-231	2 nM (95%)	17 nM (91%)
CAL51	18 nM (88%)	70 nM (45%)

In an effort to understand why **DAS-5-oCRBN** is a better degrader of c-Src compared to **DAS-CHO-5-oCRBN**, we performed biochemical and cellular binding assays with both compounds. In a biochemical activity assay, both compounds are potent binders, but in the cellular c-Src binding assay (Promega nanoBRET), **DAS-5-oCRBN** is a significantly more potent binder of c-Src. Both compounds are tight cellular binders of cereblon (Promega nanoBRET). Using the cereblon nanoBRET assay, we confirmed that the inactive control compounds (**DAS-5-oCRBN-NMe** and **DAS-CHO-5-oCRBN-NMe**) do not bind cereblon in cells (Supplementary Figure S1).

Consistent with reports of other PROTACs [25], the weak cellular binding of **DAS-CHO-5-oCRBN** (EC_{50} = 1,500 nM) but potent ability to degrade c-Src (average DC_{50} = 55 nM) demonstrates that PROTACs can act catalytically to degrade their target. Given its weak cellular binding, we wondered whether **DAS-CHO-5-oCRBN** could serve as a cellular inhibitor of c-Src. In SUM149 cells (a cell line with significant pY-419 c-Src), we found that **DAS-CHO-5-oCRBN** does not inhibit c-Src autophosphorylation at 1 μM (1 hour treatment), while **DAS-5-oCRBN** is a cellular inhibitor of c-Src (Supplementary Figure S7). This finding is consistent with the nanoBRET binding assay and demonstrates that at select concentrations (e.g., 50–100 nM) **DAS-5-oCRBN** is both an inhibitor and degrader of c-Src while **DAS-CHO-5-oCRBN** is a degrader but does not inhibit c-Src signaling at these concentrations.

Table 3. Biochemical inhibition and cellular binding of conformation-selective c-Src PROTACs.

	c-Src biochemical IC_{50}	c-Src cellular binding EC_{50}	Cereblon cellular binding EC_{50}
DAS-5-oCRBN	<30 nM	45 nM	28 nM
DAS-CHO-5-oCRBN	150 nM	1,500 nM	44 nM

Kinetics of c-Src degradation and cellular resynthesis. To better understand the kinetics of c-Src degradation, we first determined the optimal time for c-Src degradation by **DAS-5-oCRBN** and **DAS-CHO-5-oCRBN** using our c-Src ELISA and CAL148 cells (at 100 nM). We found that 18 hours of incubation with 100 nM compound was optimal for both compounds (Supplementary Figure 8).

We next wanted to determine the cellular resynthesis rate of c-Src. CAL148 cells were treated with 100 nM **DAS-5-oCRBN** 18 hours, which leads to optimal degradation of c-Src (95% of c-Src degraded, Table 2). After 18 hours, the cells were washed with fresh media and c-Src levels monitored over 4 days (96 hours). Over those 4 days, the treated cells were media exchanged every 24 hours with fresh media that contains no degrader. After 4 days, the level of cellular c-Src was 72% (compared to DMSO treated). To return to the untreated basal level of c-Src protein, our data suggest that it requires ~12 days after washout of the c-Src PROTAC (Supplementary Figure S9).

Impact of c-Src inhibitors on cellular c-Src levels. We determined the kinetics of c-Src degradation (see above) and included dasatinib and an inactive PROTAC control compound (**DAS-5-oCRBN-NMe**). With compounds that inhibit c-Src but do not degrade, we observed a marked *increase* in c-Src levels. We hypothesized this is due to feedback from c-Src inhibition and rapid translation to increase c-Src levels. To determine whether this is a general 'feature' of c-Src inhibitors, we first determined the cellular binding EC_{50} for a panel of 8 c-Src inhibitors (using the Promega nanoBRET assay). We then treated CAL148 cells with an EC_{80} concentration of each c-Src inhibitor for 18 hours and determined the c-Src protein level using our c-Src total protein ELISA. As we observed with dasatinib and **DAS-5-oCRBN-NMe**, treatment with the EC_{80} concentration for each of the 8 c-Src inhibitors leads to marked increases in c-Src levels (average = 142% c-Src, Supplementary Table S4). We observed large increases in c-Src levels regardless of which c-Src global conformation is stabilized by an inhibitor. Finally, we performed a washout experiment with dasatinib (18 hour treatment of 100 nM) and found that it required 96 hours to return to basal (100%) levels of c-Src (Supplementary Figure S10).

There was a recent report that c-Src inhibitors 'paradoxically activate' c-Src [26]. We suggest that increased levels of c-Src can contribute to c-Src pathway activation. Furthermore, the divergence between c-Src inhibitors

(which increase c-Src levels) and c-Src PROTACs (which decrease c-Src levels) represents a significant advantage of c-Src PROTACs over c-Src inhibitors.

Differential pharmacology between c-Src inhibitors and degraders. We next wanted to explore the activity of c-Src degraders in cancer cell lines known to be dependent on either c-Src activity or c-Src protein level. MDA-MB-231 cells have been reported to be growth-dependent on c-Src activity [10,17]. In contrast, CAL51 cells have been reported to be growth-dependent on c-Src protein levels and insensitive to c-Src inhibitors [17]. We treated both cell lines with siRNA targeting c-Src and confirmed that both cell lines were growth-sensitive to c-Src knockdown (Figure 7). Further consistent with literature, we found MDA-MB-231 cells were growth-sensitive to treatment of dasatinib (400 nM) but CAL51 cells were not growth-sensitive to dasatinib treatment (Figure 7). Similar to siRNA knockdown of c-Src, we found that **DAS-5-oCRBN** (400 nM) significantly reduced proliferation of both cell lines (Figure 7). Thus, we establish that c-Src PROTACs are phenotypically similar to siRNA knockdown of c-Src.

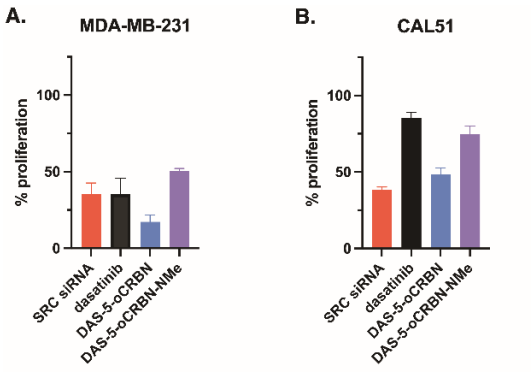

Figure 7. Knockdown versus pharmacology with c-Src degraders and inhibitors. Treatment of MDA-MB-231 cell (A.) or CAL51 cells (B.) with c-Src siRNA (SilencerSelect siRNA #sc13412, 100 nM), inhibitor (dasatinib, 400 nM), PROTAC (DAS-5-oCRBN, 400 nM), and inactive PROTAC control (DAS-5-oCRBN-NMe, 400 nM).

DAS-5-oCRBN is a better degrader of c-Src in MDA-MB-231 compared to CAL51 (per DC_{50} values, Table 2). To understand how DC_{50} values correlate to their anti-proliferative properties, we determined the GI_{50} for **DAS-5-oCRBN** in MDA-MB-231 (GI_{50} = 6 nM) and CAL51 (GI_{50} = 74 nM) cell lines using 3D cell culture (Table 4 and Supplementary Figures S11–S12). We also determined the antiproliferative properties of dasatinib, **DAS-CHO-5-oCRBN**, and the inactive (no degradation) control compounds **DAS-5-oCRBN-NMe** and **DAS-CHO-5-oCRBN-NMe** (Table 4).

Table 4. Cellular activity of dasatinib, c-Src PROTACs, and inactive control compounds.

	c-Src cellular binding EC_{50}	cereblon cellular binding EC_{50}	MDA-MB-231 GI_{50}	CAL51 GI_{50}
Dasatinib	9 nM	n.d.	12 nM	2,000 nM
DAS-5-oCRBN	45 nM	28 nM	6 nM	74 nM
DAS-CHO-5-oCRBN	1,500 nM	44 nM	62 nM	500 nM
DAS-5-oCRBN-NMe	53 nM	>10,000 nM	54 nM	3,300 nM
DAS-CHO-5-oCRBN-NMe	2,000 nM	>10,000 nM	3,000 nM	4,600 nM

Despite dasatinib being the tightest cellular binder (and a known potent cellular inhibitor) of c-Src, the c-Src degrader **DAS-5-oCRBN** is a more active antiproliferative compound in MDA-MB-231 and CAL51 cells. In the

two cell lines tested, **DAS-5-oCRBN** has a DC_{50} 4.4x lower than **DAS-CHO-5-oCRBN** which translated into an average GI_{50} that is 7x better. We observe that both c-Src degraders are more active in MDA-MB-231 over CAL51, which is consistent with their better DC_{50} values in MDA-MB-231 cells. Dasatinib and the inactive PROTACs (**DAS-5-oCRBN-NMe** and **DAS-CHO-5-oCRBN-NMe**) are inactive (>1,000 nM) in CAL51 cells consistent with their being growth-sensitive to knockdown but not inhibition of c-Src.

Conclusions.

In 2020, a dual IGF-1R/Src degrader was reported with modest c-Src degradation at 5,000 nM [27]. Here, we have developed the first potent degraders of c-Src kinase. Dasatinib is a pan-kinase inhibitor with c-Src and Abl kinases being the most potent targets [19]; however, we found that short alkyl linkers between dasatinib and thalidomide can afford higher selectivity for c-Src degradation. The geometry between the E3 ligase ligand and dasatinib, which we varied using 4- and 5-amino thalidomide, impacted selectivity for c-Src over Bcr-Abl.

We have developed one c-Src degrader (**DAS-5-oCRBN**) that is dual cellular inhibitor and a potent degrader of c-Src and Csk. **DAS-CHO-5-oCRBN** is a potent and selective degrader of c-Src that does not significantly inhibit c-Src signaling in cells. Both **DAS-5-oCRBN** and **DAS-CHO-5-oCRBN** have anti-proliferative activity in c-Src dependent cell lines with similar pharmacology to siRNA knockdown of c-Src. Our c-Src degraders represent highly valuable tools to study the differential impact of c-Src inhibition (using dasatinib or **DAS-5-oCRBN-NMe**) versus degradation (using **DAS-CHO-5-oCRBN**) versus dual inhibition/degradation (using **DAS-5-oCRBN**).

Conflicts of interest.

There are no conflicts to declare.

Acknowledgements.

This work was funded by the National Institutes of Health Grant R01 GM125881 to M.B.S.

References.

[1] R. Roskoski, A historical overview of protein kinases and their targeted small molecule inhibitors. *Pharmacol. Res.*, 2015, **100**, 1–23, DOI: 10.1016/j.phrs.2015.07.010

[2] Roskoski, R. The ErbB/HER family of protein-tyrosine kinases and cancer. *Pharmacol. Res.* **2014**, *79*, 37–74, DOI: 10.1016/j.phrs.2013.11.002

[3] Roskoski, R. Src protein-tyrosine kinase structure, mechanism, and small molecule inhibitors. *Pharmacol. Res.* **2015**, *94*, 9–25, DOI: 10.1016/j.phrs.2015.01.003

[4] Kung, J. E.; Jura, N. Structural Basis for the Non-catalytic Functions of Protein Kinases. *Structure* **2016**, *24*, 7–24, DOI: 10.1016/j.str.2015.10.020

[5] Jacobsen, A. V.; Murphy, J. M. The secret life of kinases: insights into non-catalytic signalling functions from pseudokinases. *Biochem. Soc. Trans.* **2017**, *45*, 665–681. DOI: 10.1042/BST20160331

[6] Mace, P. D.; Murphy, J. M. There's more to death than life: Noncatalytic functions in kinase and pseudokinase signaling. *J. Biol. Chem.* **2021**, *296*, 100705. DOI: 10.1016/j.jbc.2021.100705

[7] Thomas, S. M.; Brugge, J. S. Cellular functions regulated by Src family kinases. *Ann. Rev. Cell. Dev. Biol.* **1997**, *13*, 513–609. DOI: 10.1146/annurev.cellbio.13.1.513

[8] Martin, G. S. The hunting of the Src. *Nat. Rev. Mol. Cell. Biol.* **2001**, *2*, 467–475. DOI: 10.1038/35073094

[9] Ishizawae, R.; Parsons, S. J. c-Src and cooperating partners in human cancer. *Cancer Cell* **2004**, *6*, 209–214. DOI: 10.1016/j.ccr.2004.09.001

[10] Zheng, X.; Resnick, R. J.; Shalloway, D. Apoptosis of estrogen-receptor negative breast cancer and colon cancer cell lines by PTP alpha and src RNAi. *Int. J. Cancer* **2008**, *122*, 1999–2007. DOI: 10.1002/ijc.23321

[11] Finn, R. S. Targeting Src in breast cancer. *Ann. Oncology* **2008**, *19*, 1379–1386. DOI: 10.1093/annonc/mdn291

[12] Toure, M.; Crews, C. M. Small-Molecule PROTACS: New Approaches to Protein Degradation. *Angew. Chem. Int. Ed. Engl*. **2016**, *55*, 1966–1973. DOI: 10.1002/anie.201507978

[13] Lai, A. C.; Toure, M.; Hellerschmied, D.; Salami, J.; Jaime-Figueroa, S.; Ko, E.; Hines, J.; Crews, C. M. *Angew. Chem. Int. Ed. Engl.* **2016**, *55*, 807–810. DOI: 10.1002/anie.201507634

[14] Bondeson, D. P.; Smith, B. E.; Burslem, G. M.; Buhimschi, A. D.; Hines, J.; Jaime-Figueroa, S.; Wang, J.; Hamman, B. D.; Ischenko, A.; Crews, C. M. Lessons in PROTAC Design from Selective Degradation with a Promiscuous Warhead. *Cell Chem. Biol.* **2018**, *25*, 78–87. DOI: 10.1016/j.chembiol.2017.09.010

[15] Wang, Q.; Cahill, S. M.; Blumenstein, M.; Lawrence, D. S. Self-reporting fluorescent substrates of protein tyrosine kinases. *J. Am. Chem. Soc.* **2006**, *128*, 1808–1809. DOI: 10.1021/ja0577692

[16] Robers, M. B.; Vasta, J. D.; Corona, C. R.; Ohana, R. F.; Hurst, R.; Jhala, M. A.; Comess, K. M.; Wood, K. V. Quantitative, Real-Time Measurements of Intracellular Target Engagement Using Energy Transfer. *Methods Mol. Biol.* **2019**, *1888*, 45–71. DOI: 10.1007/978-1-4939-8891-4_3

[17] DepMap: The Cancer Dependency Map Project at Broad Institute: www.depmap.org (accessed May 1, 2023)

[18] Gurbani, D.; Du, G.; Henning, N. J.; Rao, S.; Bera, A. K.; Zhang, T.; Gray, N. S.; Westover, K. D. Structure and Characterization of a Covalent Inhibitor of Src Kinase. *Front. Mol. Biosci.* **2020**, *7*, 81. DOI: 10.3389/fmolb.2020.00081

[19] Lombardo, L. J.; Lee, F. Y.; Chen, P.; Norris, D.; Barrish, J. C.; Behnia, K.; Castaneda, S.; Cornelius, L. A. M.; Das, J.; Doweyko, A. M.; Fairchild, C.; Hunt, J. T.; Inigo, I.; Johnston, K.; Kamath, A.; Kan, D.; Klei, H.; Marathe, P.; Pang, S.; Peterson, R.; Pitt, S.; Schieven, G. L.; Schmidt, R. J.; Tokarski, J.; Wen, M. L.; Wityak, J.; Borzilleri, R. M. Discovery of N-(2-chloro-6-methyl- phenyl)-2-(6-(4-(2-hydroxyethyl)- piperazin-1-yl)-2-methylpyrimidin-4- ylamino)thiazole-5-carboxamide (BMS-354825), a dual Src/Abl kinase inhibitor with potent antitumor activity in preclinical assays. *J. Med. Chem.* **2004**, *47*, 6658–6661. DOI: 10.1021/jm049486a

[20] Fontana, S.; Alessandro, R.; Barranca, M.; Giordano, M.; Corrado, C.; Zanella-Cleon, I.; Becchi, M.; Kohn, E. C.; Leo, G. D. Comparative proteome profiling and functional analysis of chronic myelogenous leukemia cell lines. *J. Proteome Res.* **2007**, *6*, 4330–4342. DOI: 10.1021/pr0704128

[21] Lu, Y.; Ling, S.; Hegde, A. M.; Byers, L. A.; Coombes, K.; Mills, G. B.; Akbani, R. Using reverse-phase protein arrays as pharmacodynamic assays for functional proteomics, biomarker discovery, and drug development in cancer. *Semin. Oncol.* **2016**, *43*, 476–483. DOI: 10.1053/j.seminoncol.2016.06.005

[22] Burslem, G. M.; Ottis, P.; Jaime-Figueroa, S.; Morgan, A.; Cromm, P. M.; Toure, M.; Crews, C. M. Efficient Synthesis of Immunomodulatory Drug Analogues Enables Exploration of Structure-Degradation Relationships. *ChemMedChem*, **2018**, *13*, 1508–1512. DOI: 10.1002/cmdc.201800271

[23] Kwarcinski, F. E.; Brandvold, K. R.; Phadke, S.; Beleh, O. M.; Johnson, T. K.; Meagher, J. L.; Seeliger, M. A.; Stuckey, J. A.; Soellner, M. B. Conformation-Selective Analogues of Dasatinib Reveal Insight into Kinase Inhibitor Binding and Selectivity. *ACS Chem. Biol.* **2016**, *11*, 1296–1304. DOI: 10.1021/acschembio.5b01018

[24] Agius, M. P.; Ko, K. S.; Johnson, T. K.; Kwarcinski, F. E.; Phadke, S.; Lachacz, E. J.; Soellner, M. B. Selective Proteolysis to Study the Global Conformation and Regulatory Mechanisms of c-Src Kinase. *ACS Chem. Biol.*, **2019**, *14*, 1556–1563. DOI: 10.1021/acschembio.9b00306

[25] Bondeson, D. P.; Mares, A.; Smith, I. E. D.; Ko, E.; Campos, S.; Miah, A. H.; Mulholland, K. E.; Routly, N.; Buckley, D. L.; Gustafson, J. L.; Zinn, N.; Grandi, P.; Shimamura, S.; Bergamini, G.; Faelth-Savitski, M.; Bantscheff, M.; Cox, C.; Gordon, D. A.; Willard, R. R.; Flanagan, J. J.; Casillas, L. N.; Votta, B. J.; Besten, W. D.; Framm, K.; Kruidenier, L.; Carter, P. S.; Harling, J. D.; Churcher, I.; Crews, C. M. Catalytic in vivo protein knockdown by small-molecule PROTACs. *Nat. Chem. Biol.*, **2015**, *11*, 611–617. DOI: 10.1038/nchembio.1858

[26] Higuchi, M.; Ishiyama, K.; Maruoka, M.; Kanamori, R.; Takaori-Kondo, A.; Wantanabe, N. Paradoxical activation of c-Src as a drug-resistant mechanism. *Cell Rep.*, **2021**, *34*, 108876. DOI: 10.1016/j.celrep.2021.108876

[27] Manda, S.; Lee, N. K.; Oh, D. C.; Lee, J. Design, Synthesis, and Biological Evaluation of Proteolysis Targeting Chimeras (PROTACs) for the Dual Degradation of IGF-1R and Src. *Molecules*, **2020**, *25*, 1948. DOI: 10.3390/molecules25081948